FLAW ASSESSMENT METHODS USING FAILURE ASSESSMENT DIAGRAMS

R A Ainsworth*

The basis of failure assessment diagrams for flaw assessment is described. The practical use of failure assessment diagrams is now widespread and some advantages of the approach are discussed. More recently the approach has been extended to incorporate the influence of constraint on short-term fracture and to address creep crack growth. These extensions are briefly described and associated modifications to the shape of the failure assessment curve are illustrated.

INTRODUCTION

This paper describes methods for assessing the integrity of structures containing flaws by the use of a failure assessment diagram (FAD). Such methods were introduced by Harrison et al (1) in 1976 in the so-called R6 procedure and have been developed to the extent that R6 is now in its third revision (Milne et al (2)) and FADs have been incorporated in a British Standards Published Document PD6493 (3) and a Code Case N-494-1 (4) to the ASME Boiler and Pressure Vessel Code.

The FAD may be related to estimation schemes for J as shown by Bloom (5) and Ainsworth (6). It may also be related to crack opening displacement methods as described by Anderson (7). Although the FAD and J or crack opening displacement methods may be made equivalent, approximations are introduced in (2-4) so that the failure assessment curves are independent of geometry and/or material strain hardening

* Nuclear Electric plc, Berkeley Technology Centre, Berkeley, Glos. U.K.

properties. These approximations have been shown by Miller and Ainsworth (8) to generally introduce conservatisms and they also lead to robustness in practical use as discussed later.

In recent years, there has been considerable effort to quantify the dependence of fracture on geometry using so-called constraint parameters. These developments can be interpreted in the FAD approach by modifying the shape of the failure assessment curve as described by Ainsworth and O'Dowd (9). These modifications are summarised later in the paper.

Another recent development has been the use of FADs to assess creep crack growth under steady loading. Ainsworth (10) has derived equations which enable the fracture toughness in low temperature assessments to be replaced in the FAD approach by a material property evaluated from creep crack incubation and growth data. This use of the FAD for creep assessments is also summarised later in the paper.

THE FAD APPROACH

The FAD approach assesses fracture in terms of two parameters, here denoted K_r and L_r following (2). For applied loading of magnitude characterised by a scalar P, these are defined by:

$$K_r = K(P,a)/K_{mat} \quad (1)$$

$$L_r = P/P_L\ (a,\sigma_y) \quad (2)$$

where K is the linear elastic stress intensity factor, K_{mat} is the material fracture resistance, a is crack size and P_L is the magnitude of P at plastic collapse for a yield stress σ_y. More complex loadings, such as combined mechanical and thermal stresses, can be included in the FAD approach by modifying eqns (1) and (2).

Having evaluated K_r and L_r, failure is avoided if the point (L_r,K_r) lies within the FAD shown in Figure 1. The FAD is bounded by a failure assessment curve, $K_r = f(L_r)$, and a cut-off. The cut-off ensures avoidance of failure by plastic collapse by limiting

$$L_r \leq L_r^{max} \tag{3}$$

where L_r^{max} is defined as the ratio of the material flow stress, $\bar{\sigma}$, and the yield stress

$$L_r^{max} = \bar{\sigma}/\sigma_y \tag{4}$$

Since plastic collapse load is directly proportional to yield stress, inequality (3) combined with the definitions of eqns (2) and (4) restricts the applied load to

$$P \leq P_L\,(a,\bar{\sigma}) \tag{5}$$

The use of the flow stress in this plastic collapse limit allows for some strain hardening above the yield stress. A typical flow stress is the mean of the yield stress and the ultimate tensile stress, although R6(2) is not prescriptive about the choice of flow stress.

The failure assessment curve may be related to the results of J analysis through

$$f(L_r) = (J/J_e)^{-½} \tag{6}$$

where J and J_e are values of the J-integral obtained from an elastic-plastic analysis and an elastic analysis, respectively, both performed for the load corresponding to the value of L_r by eqn (2). As fracture is avoided if $K_r \leq f(L_r)$, the definition of eqn (1) with the failure assessment curve of eqn (3) is consistent with a fracture avoidance criterion

$$J \leq J_{mat} \tag{7}$$

where

$$J_{mat} = J_{mat}^2/E' \tag{8}$$

with E' equal to Young's modulus E in plane stress and $E' = E/(1-\nu^2)$,

where ν is Poisson's ratio, in plane strain. The value of J_e is related to K by a similar equation to eqn (8).

It can be seen from the above that the FAD approach incorporates the plastic collapse limit of eqn (5) and the elastic-plastic fracture limit of eqn (7) in a simple, visual method. This has advantages for practical use as discussed in the next section.

Equation (6) requires results of detailed analyses to construct the failure assessment curve. However, practical assessment procedures (2-4) incorporate approximate curves which enable detailed analysis to be avoided. One of these is the option 2 curve, f_2, in R6(2) which is

$$f_2(L_r) = [E\varepsilon_{ref}/\sigma_{ref} + 0.5L_r^2/(E\varepsilon_{ref}/\sigma_{ref})]^{-½} \quad (9)$$

where

$$\sigma_{ref} = L_r\sigma_y \quad (10)$$

and ε_{ref} is the uniaxial strain at the reference stress, σ_{ref}. Equation (9) is independent of geometry but dependent on material strain hardening properties. An even simpler approximate curve is that termed option 1 in R6(2) which is

$$f_1(L_r) = (1-0.14L_r^2)\,[0.3 + 0.7\exp(-0.65L_r^6)] \quad (11)$$

This curve is independent of both geometry and materials. Ainsworth (11) has shown that eqn (11) is close to the option 2 curve of eqn (9) for austenitic steels.

The FAD approach in R6 (2) has been validated for a number of large scale experiments as described by Milne et al (12). The results show that the failure assessment curves in R6 are conservative. The conservatism corresponds to factors on load-bearing capacity ranging from 1.02 to 1.45. Some of this conservatism arises from the approximations introduced in moving from eqn (6) to eqn (9) or eqn (11). However, some conservatism also arises in eqn (6) itself due to the use of highly constrained, deeply cracked bend specimens to determine fracture toughness, K_{mat} or J_{mat}. For lower constraint geometries, this conservatism can be more significant than that introduced in eqns (9) and (11), but can be removed by modifying the

FAD to allow for constraint effects as discussed later in this paper.

PRACTICAL USE OF FADS

Compared with detailed elastic-plastic analysis by the finite-element method, the FAD approaches have a number of advantages. These may be broadly categorised in terms of cost saving, ease of use, flexibility and robustness. The advantages are discussed below under these headings although it should be recognised that there is not a clear distinction between the different categories.

Cost Saving

Simplified FADs, such as eqn (9), eqn (11) or those in (4) for example, enable the user to avoid the cost of detailed elastic-plastic analysis of the cracked body. This cost saving can be significant where analyses are required for a number of load cases or crack sizes to determine margins. In probabilistic fracture mechanics assessments, where a large number of calculations need to be performed, the FAD approach is even more attractive as described by Wilson and Ainsworth (13).

The analysis requirements to follow the FAD approach are often minimal as stress intensity factor and limit load solutions are available for a wide range of geometries and crack sizes. The availability of these solutions has enabled a number of computer programs (for example, Bergman (14) and R6.CODE (15)) to be developed for performing FAD calculations. Such programs have made elastic-plastic fracture analysis almost a routine task where twenty years ago it was a major undertaking.

Another cost saving relates to material data requirements. In general, FADs require fracture toughness and stress-strain data. These are the same requirements as detailed analysis. However, with simplified failure assessment curves such as eqn (11), values of yield stress and flow stress, instead of complete stress-strain data, are sufficient. For scoping calculations or where simplified FADs demonstrate adequate margins, there is no need to go to more complex FADs and the cost of obtaining and interpreting detailed stress-strain data is avoided.

Ease of Use

As both K_r and L_r are directly proportional to load, P, the proximity of the point (L_r, K_r) to the failure assessment curve provides an immediate, visual indication of load margin. This load margin is simply the ratio OA/OB in Figure 1. This may be contrasted with detailed analysis where the difference between a calculated value of J and the material toughness, J_{mat}, provides no consistent indication of load margin due to the strong and varying dependence of J on load in the elastic-plastic regime.

Another visual aid lies in the shape of the failure assessment curve. This tends to be only weakly dependent on both geometry and material stress-strain properties as can be seen, for example, from the various curves in (4). Therefore, if a failure assessment curve is generated which looks significantly different from that in Figure 1, the user has a clear indication of a possible error in its construction. The visual indications are a strong attraction of the FAD approach and make it easy to use.

Flexibility

Although the approach has been discussed above only in terms of a single applied load, an advantage of the FAD method is that it is sufficiently flexible to be adapted in a straightforward manner to handle a number of practical issues. The R6 method (2) indicates the range of these issues: thermal and residual stresses; stable tearing; sub-critical crack growth; mixed mode loading; leak before break; probabilistic fracture mechanics; and displacement-controlled loading. More recently the approach has been extended to address constraint effects and creep crack growth as discussed later in this paper. Thus, users can apply the same basic approach to a wide range of practical problems.

Robustness

The wide range of finite-element programs, methods for calculating J, and mesh detail can often lead to very different results. On the other hand, because the input to the FAD is relatively simple the results tend to be reproducible and not subject to user interpretation. Other simplified approaches, such as the GE/EPRI estimation scheme (16), which use power-law hardening solutions are less robust. The normalised J solutions in (16) are sometimes very sensitive to the power-law used to fit the stress-strain data and to crack size, making

results user sensitive.

Thus it can be seen that the widespread use of FAD approaches has arisen for a number of reasons. The FAD is a simple, visual and robust method yet it remains sufficiently flexible for a wide range of practical issues to be treated.

EXTENSIONS FOR CONSTRAINT

To incorporate constraint effects into the FAD, it is necessary to quantify constraint in terms of the parameter L_r of eqn (2). This load dependence has been addressed in (9) for two constraint parameters: the elastic T-stress and the hydrostatic Q stress. For a single loading system, the elastic T-stress is directly proportional to load and can be written as (9)

$$T/\sigma_y = \beta_T L_r \qquad (12)$$

where β_T is a non-dimensional constraint parameter. Values of β_T are shown in Figure 2 for some common geometries for a range of crack sizes normalised by section width, or semi-width, w. For short cracks in the centre-cracked tension (CCT) geometry $\beta_T \simeq -1$. For deep cracks in bend geometries β_T is positive and small. In view of the results for the CCT geometry, $\beta_T L_r$ may be considered as a normalised measure of constraint relative to that in a shallow, centre cracked specimen at general yield.

The load dependence of the hydrostatic Q stress is more complex than the linear relationship for the elastic T-stress. The load dependence of Q has been examined in (9) for three regimes: small-scale yielding, widespread power-law plasticity; and, fully plastic behaviour. The overall dependence may be written as

$$Q = \beta_Q L_r \qquad (13)$$

where, in general, β_Q is a function of geometry, material strain hardening properties and load. Examination of detailed finite-element results in (9) for a number of geometries showed that in most cases replacing β_Q in eqn (13) by β_T provided a conservative estimate of Q. Some typical results are shown in Figure 3. However, results in (9) for a biaxially loaded centre cracked plate showed that the use of β_T in eqn (13) was

not conservative at high loads and, therefore, care must be exercised in basing assessments on T-stress calculations in all cases.

To assess constraint effects, it is necessary not only to have a measure of structural constraint, by eqns (12) or (13), but also a measure of the dependence of material toughness on constraint. In (9), this latter dependence was assessed by comparing a constraint dependent toughness K^c_{mat} with K_{mat}, the material property measured under high constraint conditions. Examination of cleavage and ductile fracture toughness data showed that these could be approximately related for negative constraint by

$$K^c_{mat} = K_{mat}[1 + \alpha(-\beta L_r)^p] \qquad (14)$$

where α,p are constants and β represents either β_T or B_Q depending on the constraint parameter adopted. Values of p = 1-2 with α typically about unity were found in (9). For positive constraint, $K^c_{mat} \simeq K_{mat}$. The form of eqn (14) is used here to illustrate constraint based modifications to the failure assessment curve. However, the modifications could similarly be developed for other forms provided the relationship between K^c_{mat} and K_{mat} is expressed as a function of constraint.

To address constraint effects, eqn (7) is assumed to be replaced by

$$J \leq J^c_{mat} \qquad (15)$$

Since J can be estimated using eqn (6) and J^c_{mat} is related to J_{mat} by the J-equivalent of eqn (14), the failure avoidance criterion of inequality (15) can be written

$$K/K_{mat} \leq f(L_r)\,[1 + \alpha\,(-\beta L_r)^p] \qquad (16)$$

This is equivalent to retaining the definition of K_r by eqn (1) in terms of a fracture toughness derived from a highly constrained geometry but with the failure assessment curve being replaced by a constraint based curve, f_c,

$$f_c = f(L_r)\,[1 + \alpha\,(-\beta L_r)^p] \qquad (17)$$

Modifications to the option 1 curve of eqn (11) have been illustrated in (9) for both a linear (p = 1) and a quadratic (p = 2) fit to toughness data. The quadratic fit is shown here in Figure 4. At very low values of L_r/K_r, there is no effect of constraint and the failure assessment curves all converge to $K_r = 1$. Very low values of L_r/K_r can be achieved by increasing specimen size and this leads to reducing $|T|$ for a given value of K. Consequently, as $L_r/K_r \rightarrow 0$ then $T/K \rightarrow 0$ and similarly $Q \rightarrow 0$. Thus, the extreme left hand side of the FAD corresponds to high constraint irrespective of geometry.

In the small-scale yielding regime ($L_r \leq 0.5$), the failure assessment curve is sensitive to constraint and is also sensitive to the position of the failure assessment point. Under widespread yielding conditions, the effects of constraint on load factors (see Figure 1) are lower than in the small-scale yielding regime because of the stronger load dependence of J as reflected in the shape of the failure assessment curve under widespread plasticity.

It can be seen that a framework has been developed for including constraint effects through modifications to the shape of failure assessment curves without any changes to the definitions of K_r and L_r. Generally, the modifications require a geometry and crack size dependent parameter to quantify structural constraint and parameters (α,p) relating the fracture toughness in a shallow, centre cracked tension geometry at general yield to the fracture toughness in a deeply cracked bend specimen.

EXTENSION TO CREEP CRACK GROWTH

Recently, the FAD approach has been examined in detail (10) to see how the various input parameters can be modified to enable its use at high temperature. The strong similarity between reference stress methods for estimating J via eqn (9) and the corresponding methods for estimating the high temperature crack tip parameter C* has been used to develop a FAD approach. This can be used to guard against crack initiation or small amounts of creep crack growth in a particular time, t. The failure assessment curve is identical to eqn (9) but the value of σ_y used to derive the reference stress from eqn (10) is the (proof) stress to 0.2% inelastic strain evaluated from isochronous stress-strain data for the time at which an assessment is required. Similarly, ε_{ref} is the strain at the reference stress obtained from isochronous data. At long times, this is dominated by creep strains. At short times, it is shown in (9) that the inclusion of elastic strain in ε_{ref} covers transient effects in the

stress redistribution period following initial loading.

Failure assessment curves are shown in Figure 5 for austenitic steel at 600°C using eqn (9) and average isochronous curves. Also shown is the option 1 curve of eqn (11). In the absence of creep, the failure assessment curve of eqn (9) is very close to the option 1 curve. At low values of L_r, the failure assessment curves fall increasingly below the curve for t = 0 with increase in time. It appears that the curves are not strongly dependent on time and the curve for the longest time could be used for conservative assessments at shorter times.

For creep assessments, the cut-off L_r^{max} is not given by eqn (4) but is defined as the ratio of the stress to rupture for the assessment time divided by the 0.2% proof stress evaluated from isochronous data, also at the assessment time. This ensures that failure by continuum damage mechanisms is avoided (10).

The main problem for high temperature assessments is to derive a value of K_{mat} to define K_r by eqn (1). Conventionally, creep crack incubation and growth data are presented in terms of C* by equations such as

$$t_i \, C^{*\phi} = B \tag{18}$$

$$\dot{a} = AC^{*q} \tag{19}$$

where t_i is the time before creep crack growth starts, $\dot{a}$ is creep crack growth rate and B, ϕ, A, q are material- and temperature-dependent constants. In reference (10) it was shown that a pseudo toughness, K_{mat}, to be used in the FAD approach could be related to these constants by

$$K_{mat} = [EB^{1/\phi} \, t^{-(1/\phi - 1)}]^{1/2} \tag{20}$$

to avoid initiation in time t, and

$$K_{mat} = [E(\Delta a/A)^{1/q} \, t^{-(1/q-1)}]^{1/2} \tag{21}$$

to avoid a small amount of crack growth, Δa, in time t. Equation (21)

assumes that crack growth starts at t = 0 but it is possible to define K_{mat} allowing for both initiation and growth (10). The toughness defined by eqns (20) and (21) reduces with increasing assessment time. More recently, Hooton et al (17) have shown that values of K_{mat} can also be derived directly from displacement data obtained during a creep crack growth test, thus avoiding the intermediate step of interpreting results in terms of C* by eqn (18) or eqn (19).

Thus it can be seen that failure assessment diagrams can be used to guard against creep crack initiation or small amounts of creep crack growth. The failure assessment curves do depend on creep deformation behaviour as represented by isochronous data but the general shape is not that different from the low temperature curves. Whereas the cut-off, L_r^{max}, guards against plastic collapse at low temperatures, at high temperatures it guards against creep rupture by continuum damage processes. The approach is not as well developed as the FAD method at low temperature, particularly as creep crack initiation and growth data are not generally available in the form of a toughness K_{mat}. However, the advantages of the FAD approach discussed earlier also apply at high temperatures and, therefore, it is expected that the FAD for creep assessment will gain increased use in the future.

ACKNOWLEDGEMENT

This paper is published with permission of Nuclear Electric plc.

REFERENCES

(1) Harrison, R.P., Loosemore, K. and Milne, I., "Assessment of the Integrity of Structures Containing Defects", Central Electricity Generating Board, U.K., Report No. R/H/R6, 1976.

(2) Milne, I., Ainsworth, R.A., Dowling, A.R. and Stewart, A.T., Int. J. Pres. Ves. Piping, Vol. 32, 1988, pp.3-104.

(3) British Standards Institution, "Guidance on Methods for Assessing the Acceptability of Flaws in Welded Structures", Published Document PD6493, 1991.

(4) American Society of Mechanical Engineers, "Pipe Specific Evaluation Procedures and Acceptance Criteria for Flaws in Class 1 Ferritic Piping that Exceed the Acceptance Standards of IWB-3514.2", ASME Boiler and Pressure Vessel Code, Section XI, Division 1, Case N-494-1, 1992.

(5) Bloom, J.M., ASTM STP 803, 1984, pp. II.206-II.238.

(6) Ainsworth, R.A., Engng. Fract. Mech., Vol. 19, 1984, pp. 633-642.

(7) Anderson, T.L., "Fracture Mechanics Fundamentals and Applications", CRC Press. Boston, USA, 1991.

(8) Miller, A.G. and Ainsworth, R.A., Engng. Fract. Mech., Vol. 32, 1989, pp. 233-247.

(9) Ainsworth, R.A. and O'Dowd, N.P., "A Framework for Including Constraint Effects in the Failure Assessment Diagram Approach for Fracture Assessment", Nuclear Electric plc, U.K., Report No. TIGM/REP/0097/93, 1993.

(10) Ainsworth, R.A., Fatigue Fract. Engng. Mater. Struct., Vol. 16, 1993, pp.1091-1108.

(11) Ainsworth, R.A., "Failure Assessment Diagrams for Use in R6 Assessments of Austenitic Components", Conference on Fracture in Austenitic Components, CEA Saclay, Paris, 1991.

(12) Milne, I., Ainsworth, R.A., Dowling, A.R. and Stewart, A.T., Int. J. Pres. Ves. Piping, Vol. 32, 1988, pp.105-196.

(13) Wilson, R. and Ainsworth, R.A., "A Probabilistic Fracture Mechanics Assessment Procedure" in SMiRT 11 Transactions, Tokyo, Japan, Vol. G, 1991, pp.325-330.

(14) Bergman, M., "En Metod för Säkerhetsbedömning av Komponenter med Sprickor - Manual för Datorprogram", The Swedish Plant Inspectorate, Sweden, Report No. SA/FoU-90/02, 1990.

(15) R6.CODE, User Manual, Nuclear Electric plc, U.K., 1994.

(16) Kumar, V., German, M.D. and Shih, C.F., "An Engineering Approach to Elastic-Plastic Fracture analysis", Electric Power Research Institute, U.S.A., Report No. NP-1931, 1981.

(17) Hooton, D.G., Green, D. and Ainsworth, R.A., "An R6 Type Approach for the Assessment of Creep Crack Growth Initiation with Validation using 316L SS Test Specimens", To be presented at ASME Pressure Vessels and Piping Conference, Minneapolis, U.S.A., 1994.

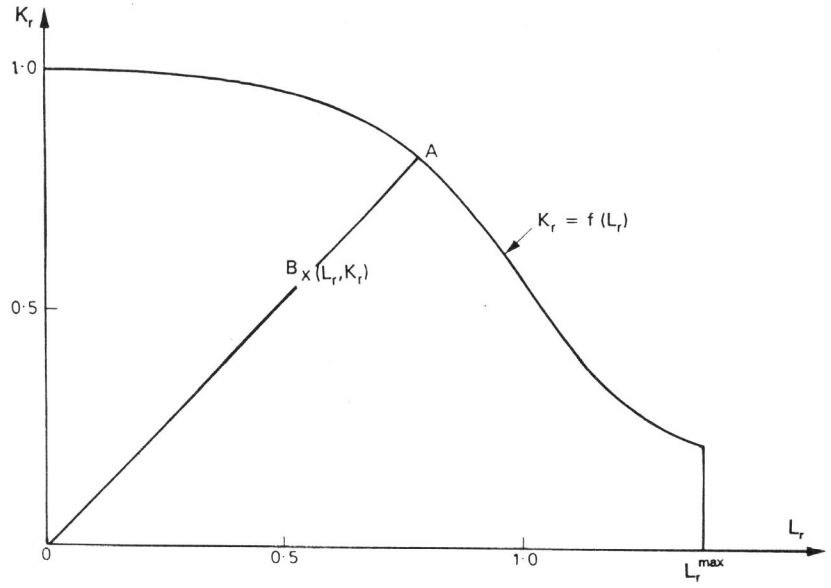

Figure 1 The basic failure assessment diagram

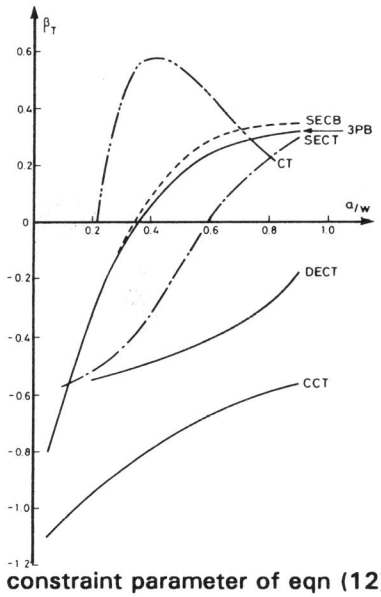

Figure 2 Elastic constraint parameter of eqn (12) for common test specimen geometries

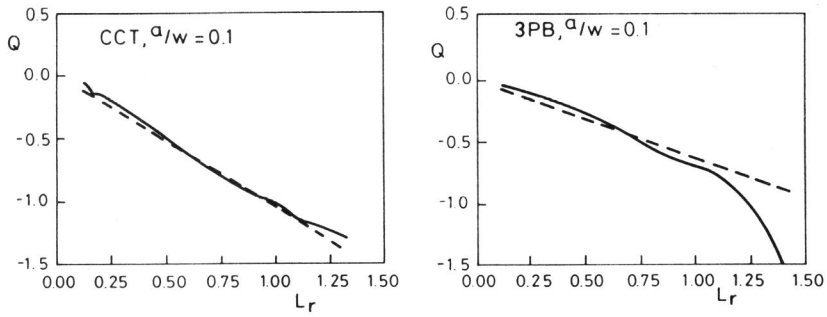

Figure 3 Hydrostatic Q stress as a function of load parameter L_r

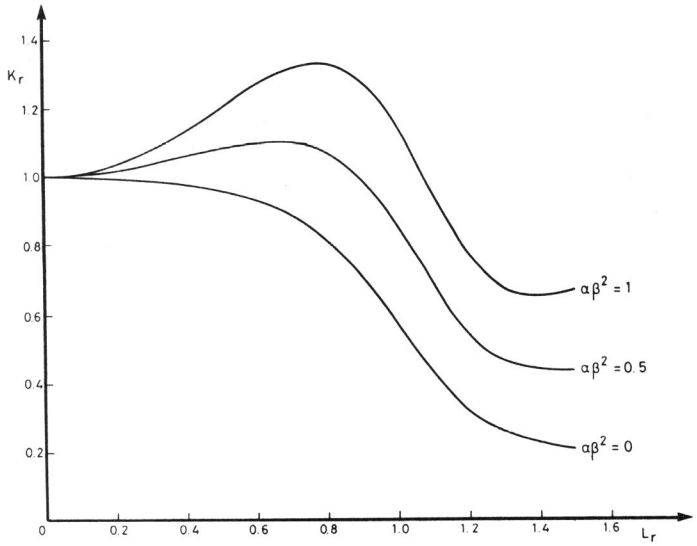

Figure 4 Modified failure assessment curves using eqn (17) with p = 2

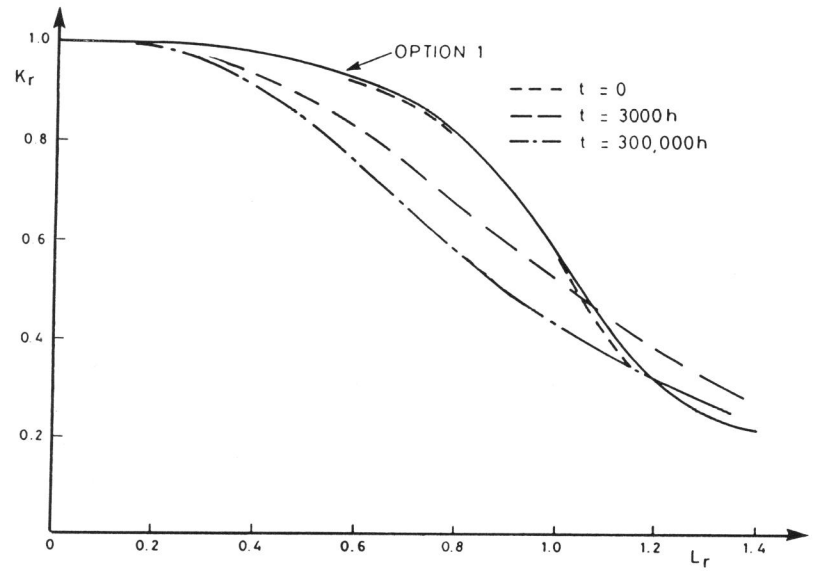

Figure 5 Failure assessment curves for austenitic steel at 600°C